PCCP

Accepted Manuscript

ROYAL SOCIETY OF CHEMISTRY

www.rsc.org/pccp

Electrochemical Activation of Commercial Polyacrylonitrile-based Carbon Fiber for Oxygen Reduction Reaction†

Haibo Xu, Guangsen Xia, Haining Liu, Shuwei Xia and Yonghong Lu*

Key Laboratory of Marine Chemistry Theory and Technology, Ministry of Education; College of Chemistry and Chemical Engineering, Ocean University of China, Qingdao 266100, P.R. China.

*Corresponding Author E-mail: lazake@163.com

Received (in XXX, XXX) Xth XXXXXXXXX 20XX, Accepted Xth XXXXXXXXX 20XX

DOI: 10.1039/c00000000a

Abstract

Nitrogen (N)-doped carbon and its non-noble metal composite replacing platinum-based oxygen reduction reaction (ORR) electrocatalysts still have some fundamental problems remained. Here the micron-sized commercial polyacrylonitrile-based carbon fiber (PAN-CF) electrode was modified by electrochemical method, converting its inherent pyridinic-N into 2-pyridone (or 2-hydroxyl pyridine) functional group existing in three-dimensional active layers with remarkable ORR catalytic activity and stability. Carbon atom adjacent to nitrogen and oxygen atom is prone to acting as an active site to efficiently catalyze a two-electron ORR process. However, after coordinating pyridone to Cu^{2+} ion, together with the electrochemical reaction, the chemical redox between Cu^{+} and ORR intermediates synergistically tends to a four-electron pathway in alkaline solution. In different medium, the complexation and dissociation can induce the charge transfer and reconstruction among proton, metal ion and pyridone functionalities, eventually leading to the changes of ORR performance.

Broader context

Oxygen reduction reaction (ORR) is widely applied in both energy conversion devices (e.g., fuel cells, metal-air batteries) and environmental pollution control, which are serious challenges humanity will face for a long time. Four-electron ORR is mainly used as cathode reaction for energy storage devices (fuel cells, metal-air batteries, *etc*), while two-electron ORR is mainly for continuous in-situ generation of H_2O_2 in electro-Fenton process to degrade refractory pollutants. It is of great significance to investigate and control the selectivity of cathode materials for specific application. Here, we report for the first time that polyacrylonitrile-based carbon fiber (PAN-CF) was electrochemically activated, obtaining obviously enhanced ORR activity. We reveal that the ORR selectivity can be regulated from $2e^-$ to $4e^-$ pathway by forming one or two adjacent active site(s) in different medium. Thus, the systematical ORR mechanisms are useful for future design and preparation of catalyst and electrode.

Introduction

High efficient oxygen reduction reaction (ORR) of four- or two-electron ($4e^-$ or $2e^-$) pathway is of great value in a variety of applications such as the clean power generation in proton exchange membrane fuel cell (PEMFC), [1-3] metal-air batteries, [4, 5] the great reduction of energy consumption in chlor-alkali industry *via* replacing hydrogen-evolving cathode with an air cathode, [6, 7] the yield of H_2O_2 on line[8] and efficient degradation of persistent organic pollutants (POPs) *via* electro-Fenton process, [9] *etc*.

Platinum (Pt) has been considered as the most efficient electrocatalyst for $4e^-$ ORR in fuel cells but with very high cost. Therefore, besides a large amount of research on improving Pt-based electrocatalysts, [10,11] various non-noble metal alternative catalysts like metal-N_4 complexes (metal porphyrins, metal phthalocyanine), transition metal oxides and chalcogenides, N-doped carbon (carbon nanotube, graphene, fiber, nanocage, *etc*) have been developed. [2, 12-15] Among them, N-doped carbon and its non-noble metal composite are the most promising. [16, 17] However, the stability, durability, activity and cost of these materials for ORR are still inferior compared to Pt-based catalysts and unable to meet the demand of practical applications. [2, 18] Besides, these researches mainly focus on nano-scale materials via complex preparation procedure, and many controversies over the mechanism still remain, such as the categories of nitrogen groups, the roles of the medium and non-noble metal, and the correlation of N-doping structure with ORR performance, the corresponding research on micro-scale ones is far less enough yet. [19-25]

Commercially available polyacrylonitrile-based carbon fiber (PAN-CF) is a micro-sized N-containing carbon material (N content: 2~6 wt.%) *via* high-temperature carbonization (1200~1600 □), [26] its low price and high electrical conductivity and structural stability have attracted much interest in flow batteries, [27] the dissolved oxygen seawater battery (SWB), [28, 29] *etc*. However, the poor ORR performance of PAN-CF cathode resulting in a low volume specific power of SWB (~ 2.7 mW L^{-1}) has hampered its widespread use. Therefore, in this study, we intend to enhance the ORR activities of PAN-CF electrode *via* electrochemical modification, and reveal the mechanism for future design and preparation of catalyst and electrode.

Results and discussion

The commercial PAN-CF was activated by recurrent galvanic pulses in H_2SO_4, and similar to the modified graphite electrode (MGE), [30, 31] to obtain the modified PAN-CFs (MPAN-CFs, denoted as P.125,

P.25, *etc,* in terms of activation current density of 0.125, 0.25 A g^{-1}, *etc*) (Fig. S1). It is worth noting that alike MGE, pseudo-capacitive characteristic attributed to the surface O-containing groups could also be observed on MPAN-CFs (Fig. 1a). Comparably, the ORR current density (*i.e.* plateau value in Fig. 1c) of N-free MGE was far lower than those of MPAN-CFs, while the ORR current density and pseudo-capacitance of MPAN-CFs increased with increasing activation strength (P2.5 had nearly the same ORR current density as P4 and the fiber wire was found easily break or lose electrochemical performance beyond 5 A g^{-1} of activation current density); and the worst of all, PAN-CF showed neither capacitive character nor ORR activity. Additionally, we modified PAN-CF by chemical oxidation in molten sodium nitrate ($NaNO_3$) at 400 ℃ (denoted as P-MS), it exhibited small double-layer capacitance (Fig. 1b) and however notable ORR current density (Fig. 1d). As a consequence, the results indicate that O-containing groups alone have poor ORR activity and the inherent N in PAN-CF is converted into N-containing groups with high ORR activity via chemical or electrochemical activation.

Although the smooth surface and apparent diameter of PAN-CF changed little under scanning electron microscope (SEM), the original turbostratic graphite structure was indeed further damaged by electrochemical activation, inferring from the broadening and weakening of the diffraction peak at 2θ = 25.6° (002) in X-ray diffraction (XRD) and the increasing intensity ratio of D to G peak (I_D/I_G) in Raman spectroscopy with the increase of activation intensity (Fig. S2). Besides, the Brunauer-Emmett-Teller (BET) specific surface area doubled only from 0.537 to 1.058 m^2 g^{-1}. All indicate the electrochemical activation has an advantage of mildly adding surface defects but bringing no obvious damage to surface morphology.

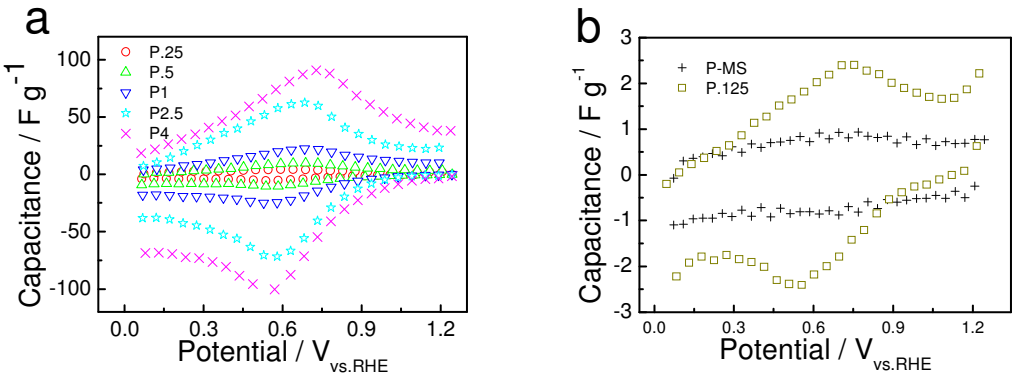

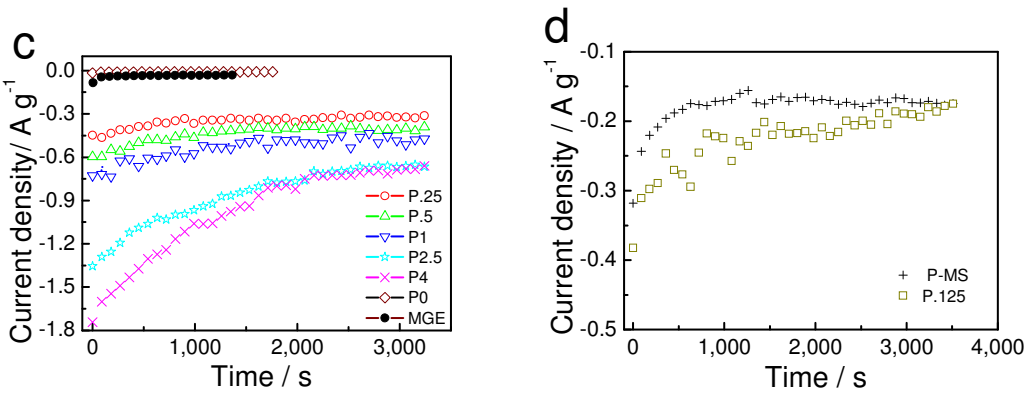

Fig. 1 CV capacitance vs. potential curves for (a) MPAN-CFs (P.25, P.5, P1, P2.5 and P4) , (b) P-MS and MPAN-CF (P.125) in deaerated 2 mol L^{-1} H_2SO_4. Current density vs. time curves for (c) MGE, PAN-CF (P0), P.25, P.5, P1, P2.5 and P4, (d) P-MS and P.125 at 0.33 V under magnetically stirring of 600 r.p.m. in naturally aerated pH8.2 seawater. P-MS exhibited nearly the same ORR current density but a far less capacitance as P.125.

Surface chemical compositions of PAN-CF before and after activation were analyzed, and they were subsequently ion-sputtered for 100 s to conduct an in-depth profile analysis by X-ray photoelectron spectroscopy (XPS). Compared with PAN-CF surface, O and N content evidently increased both on surface and in ion-sputtered profile of MPAN-CFs (Table S1), and the rise of N content definitely comes from the surface enrichment of inherent N by electrochemical/chemical oxidization and etching action. However, the contents of O and N seemed no direct correlation with ORR activity and pseudo-capacitance shown in Fig. 1. Fitting C1s spectra (Table S2), 284.3 and 285.2 eV represent the functionalized sp^2 and sp^3 C-C bond on defect sites, respectively, and the ratio of their total sum to the content of non-functionalized sp^2 C-C bond at 284.6 eV reflects the degree of defects and the proportion of disordered carbon.[32] As a result, the much higher surface ratios (>4) and in-depth ratios (>3) of MPAN-CFs than PAN-CF surface ratio (1.8) indicate a remarkable increase of defects from surface to deep profile after activation. Furthermore, these in-depth ratios depended on the activation intensity, the higher the activation current density the higher the in-depth ratios, indicative of a thicker three-dimensional active layer.

Fitting N1s spectra (Fig. S3), pyridinic-N, graphitic-N and pyridine-N-oxide existed on PAN-CF surface, consistent with literatures.[33, 34] After activation, unstable pyridine-N-oxide completely disappeared and surprisingly, pyridinic-N only remained in ion-sputtered profile; simultaneously, a pair of intense peaks

at 399.4 and 400.2 eV appeared, which were ever ascribed to pyrrolic-N/pyridone, [32, 35] but in our work they solely correspond to pyridone due to the absence of pyrrolic-N in PAN-CF. [33, 34] And more importantly, a decrease in pyridinic-N was markedly associated with an increase in pyridone, a N- and O-doped functional group (Fig. 2). Considering the little change of stable graphitic-N and the 1/2~2/3 more pyridone in total N, thereby newly generated pyridone is taken for granted as the fundamental reason for the enhancement of ORR activity.

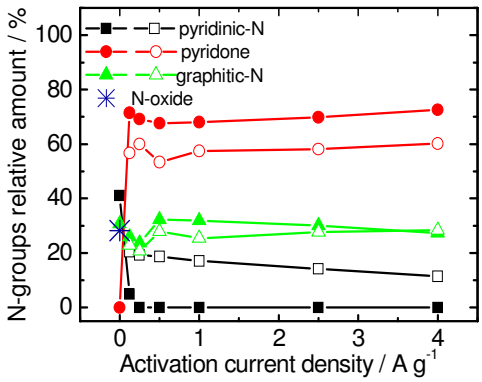

Fig. 2 Changes in relative amount of different N-groups on PAN-CF and MPAN-CFs surface (filled symbols) and in their 100s-ion-sputtered profile (unfilled symbols) with the activation current density.

Accordingly, an ortho-selectively nucleophilic substitution reaction probably occurs during electrochemical oxidation shown in eq. (1), *i.e.* pyridinic-N is changed into 2-pyridone or 2-hydroxyl pyridine, a pair of tautomeric compound corresponding to pyridone ring of amide-type at 399.4 eV or imide alcohol-type at 400.2 eV. Recently, Achour *et al* also obtained pyridone from pyridinic-N by electrochemical anodic oxidation of N-doped carbon nano-wall films. [36] Silva R. *et al* observed the high ORR activity from N- and O-doped meso-porous carbons. [37]

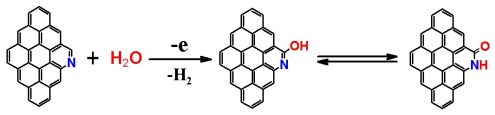

(1)

Subsequently, the influence of the electrolyte medium and metal ion on ORR properties of MPAN-CFs is investigated in detail. As a whole, ORR onset potential (the separate points of two potential~time curves under nitrogen- and oxygen-saturated condition) moved positively with the increase of medium pH (Fig.

S4), indicative of a better activity in alkaline solution. Two plateau onset potentials at 0.91 V in alkaline solution as well as 0.61 V in acidic solution arose at both ends; and compared with the reported Pt/C, [38] a small potential difference of *ca.* 0.1 V also confirms an excellent ORR activity of MPAN-CF in alkaline solution. Next, a MPAN-CF was immersed into the saturated $CuCl_2$ solution to prepare a composite electrode (denoted as MPAN-CF-Cu(II)) through Lewis acid-base reaction, and its CV characteristics were compared with those of PAN-CF and MPAN-CF in H_2SO_4, Na_2SO_4 and KOH (Fig. 3a-c). In fact, aside from the wide pseudo-capacitive redox peaks in all electrolytes, MPAN-CF-Cu(II) newly showed a pair of Cu(II)/Cu(I) redox peaks whose reduction peak potential is at 0.7 V in alkaline and 0.4 V in neutral solution (arrows in Fig. 3b and c). At the same time, on polarization curves (Fig. 3d-f), MPAN-CF-Cu(II) had the highest polarization current density and the most positive onset potential, *i.e.* the best activity in all conditions, which may be attributed to the complexation of pyridone with Cu^{2+} that changes the ORR selectivity to reduce the molecular O_2 more completely and to enhance the ORR activity subsequently. In a word, as for the ORR activity, MPAN-CF-Cu(II) is the best in terms of electrode, and the alkaline solution is the best in terms of medium.

Additionally, ORR selectivity of MPAN-CF and MPAN-CF-Cu(II) was evaluated by the current efficiency (CE) of H_2O_2 yield. H_2O_2 was detected by titanium potassium oxalate ($C_4K_2O_9Ti$) spectrophotometry method instead of conventional rotating ring disk electrode (RRDE) used by nano-sized materials. [39] To meet the requirements of detection limit and stability, the CE of H_2O_2 yield had to be measured at high cathodic overpotential in short time (the red filled triangles in Fig. 3d-f). In acidic solution, both MPAN-CF and MPAN-CF-Cu(II) (the least point for poor stability) exhibited a predominant $2e^-$ pathway. In alkaline solution, MPAN-CF was dominated by $2e^-$ process whereas MPAN-CF-Cu(II) revealed a $4e^-$ one at potentials negative than 0.7 V with the ORR current up to 0.54 A m^{-2} (relative to the BET specific surface area) at 0.7 V. Moreover, in neutral solution, the mixed $2e^-$ and $4e^-$ reduction process for MPAN-CF and the dominant $4e^-$ process for MPAN-CF-Cu(II) occurred at potentials negative than 0.4 V. Similarly, the MPAN-CF-Fe(III) by coordinating pyridone to Fe^{3+} also confirmed that the complexation and dissociation of pyridone with proton (acidic solution) or metal ion in different medium changed the ORR activity and selectivity (Fig. S5). Finally, a 650-hour performance test of MPAN-CF-Cu(II) at 0.33 V in pH8.2 seawater was investigated. After an expectedly gradual dissociation of Cu^{2+}, the ORR current

density kept constant at *ca.* 0.67 A g^{-1} after 36 h, signaling the excellent long-term stability of MPAN-CF itself (Fig. S6).

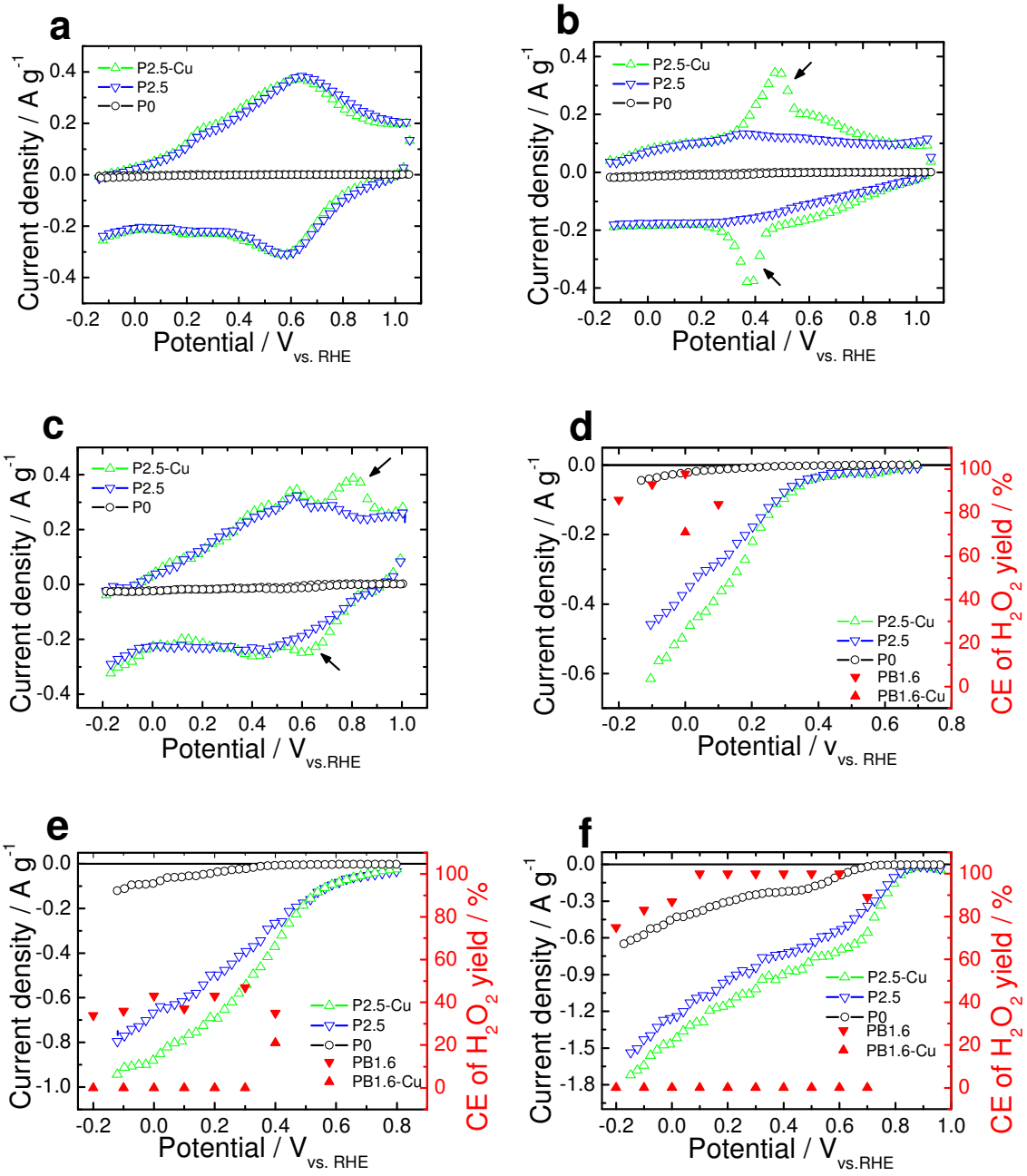

Fig. 3 (a-c) Cyclic voltammetry curves under deaerated conditions; (d-f) polarization curves under magnetically stirring of 600 r.p.m. in naturally aerated solutions for PAN-CF (P0), MPAN-CF (P2.5) and MPAN-CF-Cu(II) (P2.5-Cu) with scan rate of 5 mVs^{-1}, and current efficiency (CE) of H_2O_2 yield (the red filled triangles in d-f) at different applied potentials under air-aeration condition for MPAN-

CF (PB1.6) and MPAN-CF-Cu(II) (PB1.6-Cu) in 0.5 mol L^{-1} H_2SO_4 (a and d), 0.5 mol L^{-1} Na_2SO_4 (b and e) and 0.1 mol L^{-1} KOH (c and f).

To associate ORR performance with N-doping structure, density functional theory (DFT) calculation was carried out to simulate the optimal structure and surface charge distribution (Fig. 4, Fig. S7). N-containing groups are believed to randomly disperse on edge plane, [40] here the positive charge density on 2C of pyridone (carbon atom adjacent to N and O) is evidently much higher than that of either pyridinic- or graphitic-N (carbon atom adjacent to N), thus it is identified as the active site derived from the strong electron affinity of both N and O. [19, 38] After the complexation of protonated pyridone with Cu^{2+} in acidic solution, a large difference of bond length between Cu^{2+} with N and O (1.971 and 2.609 Å) exists, and the positive charge density on Cu^{2+} was 0.639, while those in neutral/alkaline solution were 2.022 Å, 2.177 Å and 0.495 respectively (Fig. 4d and e), meaning apparently different bond number, bond strength and charge density. The different complexation strength may change the reduction capability of metal ion, the weak complexation from one bond makes it reduced at more negative potential while the strong complexation from two bonds favors losing or receiving the electron and therefore makes metal ion reduced at more positive potential. That is to say, one bond between Cu^{2+} and N in acidic solution and the two bonds between Cu^{2+} with N and O in neutral/alkaline solution resulted in the different charge density, which probably changed the redox potential of Cu(II)/Cu(I) complex in Fig. 3a-c and the ORR selectivity in Fig. 3d-f.

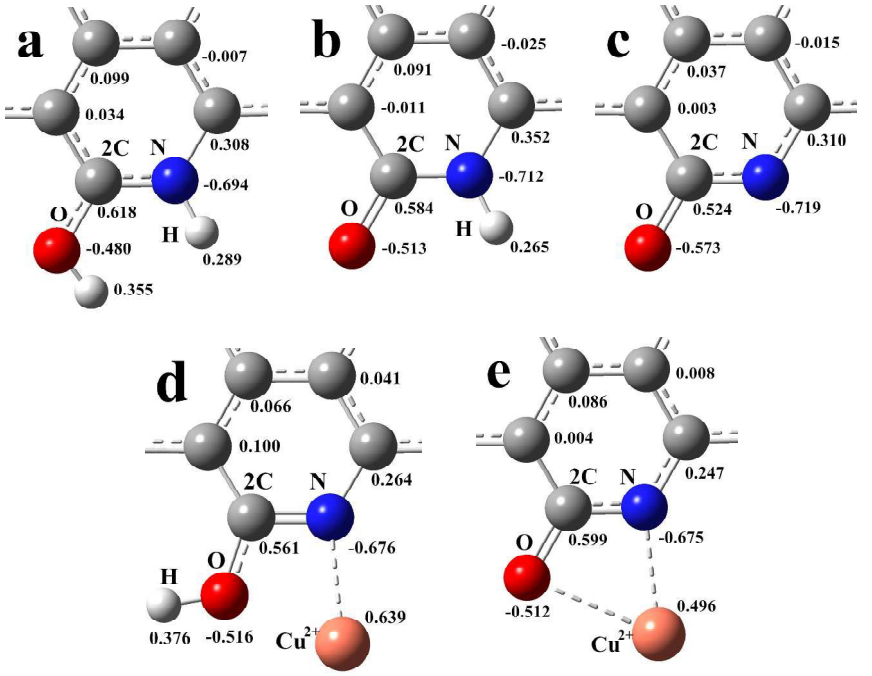

Fig. 4 Surface charge distribution on (a) protonated pyridone and (d) protonated MPAN-CF-Cu(II) in acidic solution, (b) pyridone in neutral solution, (c) deprotonated pyridone in alkaline solution and (e) MPAN-CF-Cu(II) in neutral and alkaline solution.

As for the effect of surface charge transfer and reconstruction on ORR selectivity, take MPAN-CF and MPAN-CF-Cu(II) in alkaline solution as an example. In Fig. 5a, molecular O_2 is polarized in outer Helmholtz layer over a long range and generated HOO after gaining an electron, [41] HOO is preferentially adsorbed on 2C atom to form HOO*. Considering the bond length of C-O* (1.469 Å) is longer than that of O-O* (1.459 Å), C-O* bond breaks more easily to form HO_2^- in the reduction process of C-O*OH, resulting in a typical $2e^-$ pathway. In Fig. 5b, MPAN-CF-Cu(II) complex easily gains an electron to form MPAN-CF-Cu(I) complex according to the distinct redox peaks in Fig. 3c, and HOO by reduction of O_2 is similarly adsorbed on 2C to form HOO*. It is notable for Cu^+, a small interatomic distance of 2.487 Å between it and O in HOO* and the decline of charge density from 0.411 to 0.357 will probably facilitate the intra-molecular chemical redox reaction: *i.e.* Cu^+ is oxidized into Cu^{2+} with a reasonable rise of charge density to 0.473 again, and the O-O* bond simultaneously breaks to form OH^- and C-O*H which is subsequently electrochemically reduced into OH^-, too. Namely, Cu^{2+} and 2C in MPAN-CF-Cu(II) complex are considered the two adjacent active sites with a tendency of $4e^-$ selectivity, and an

electrochemical/chemical synergetic effect between metal ion and oxygen reduction intermediate favors the $4e^-$ pathway, similar to the ORR acceleration by a coupled electrochemical/chemical process on copper in H_2SO_4. [42] In brief, a single active site from 2C atom in pyridone favors a $2e^-$ pathway and the two adjacent active sites from 2C and metal ion facilitate a $4e^-$ pathway and the best activity.

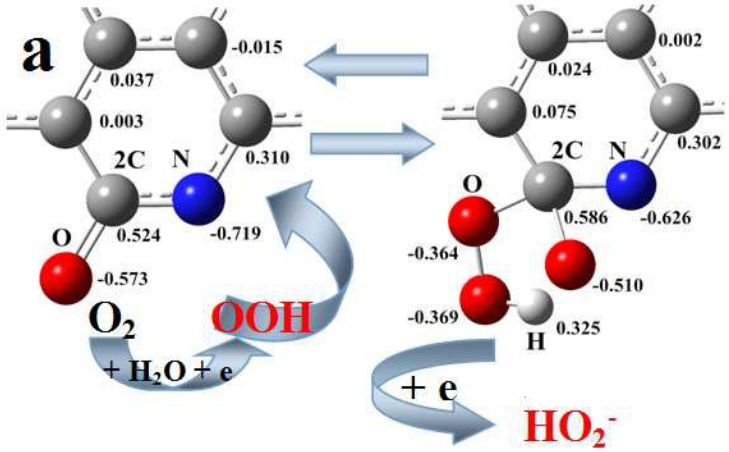

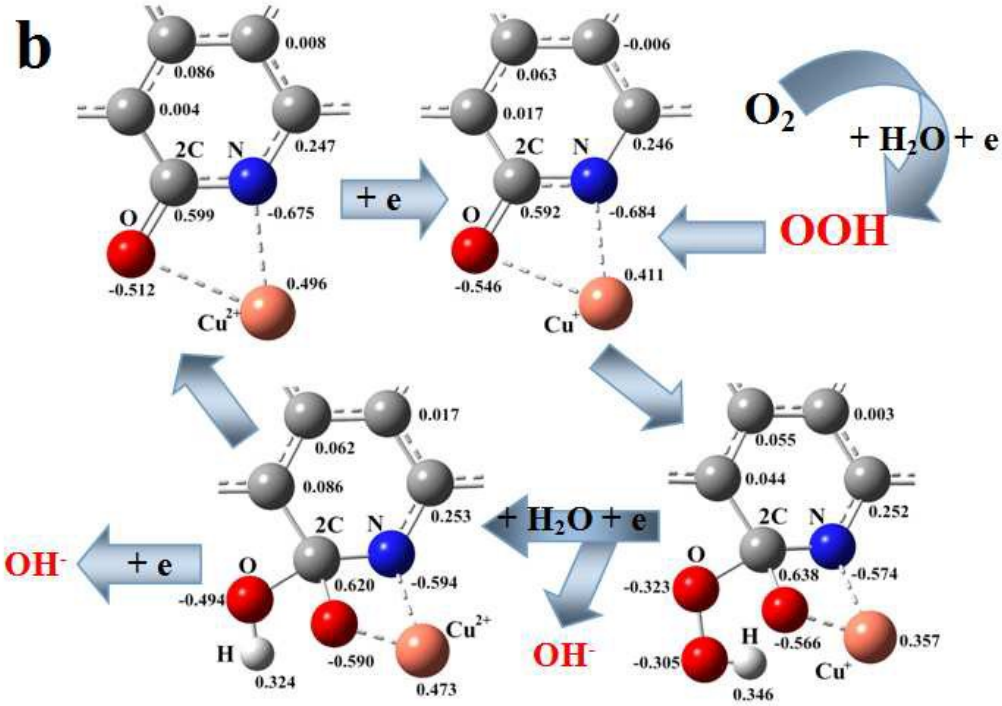

Fig. 5 Schematic diagram of (a) $2e^-$ pathway of MPAN-CF and (b) $4e^-$ pathway of MPAN-CF-Cu(II) in alkaline solution.

Apart from the predominant active site of 2C, the 6C atom in pyridone (connecting with N) can presumably act as another adsorption active site, whose net positive charge density of 0.352 in neutral solution is the highest compared with others (0.303 in acidic and 0.310 in alkaline solution) in Fig. 4, that may explain why MPAN-CF displayed the mixed $2e^-$ and $4e^-$ selectivity in neutral solution (Fig. 3e and Fig. S7).

Conclusions

A low-cost MPAN-CF electrode was obtained by electrochemically modifying micro-scale PAN-CF. The degree of defects and thickness of active layer in MPAN-CF increased dependent on the activation intensity, and the newly generated pyridone in three-dimensional active layers was considered responsible for high ORR activity and stability. Moreover, ORR activity and selectivity of MPAN-CF were influenced by the medium and metal ion. In alkaline solution, two adjacent active sites from metal ion and carbon atom connecting with N and O facilitated the $4e^-$ selectivity as well as the best activity, and an electrochemical/chemical synergetic mechanism between metal ion and oxygen reduction intermediate was proposed to correlate the structure of composite with ORR performance.

Acknowledgments

This work was supported by National Major Scientific Instruments Development Project of the National Natural Science Foundation of China (41427803), Shandong Province Science and Technology Development Plan (2014GHY115036) and Special Foundation of Ocean University of China (201022006).

Notes and references

†Electronic Supplementary Information (ESI) available: [Experimental details, supplementary Figs. S1-S7 and Tables S1-S2, including electrode and system arrangement; XRD patterns and Raman spectra of PAN-CF and MPAN-CFs; N-containing groups analysis by XPS; ORR activity influenced by medium pH; ORR activity and selectivity for MPAN-CF-Fe(III); durability test; quantum mechanics calculation; element analysis of C,O and N; carbon species analysis by XPS]. See DOI: 10.1039/c00000000a.

1. Y. Bing, H. Liu, L. Zhang, D. Ghosh and J. Zhang, *Chem. Soc. Rev.*, 2010, **39**, 2184.
2. Z. Chen, D. Higgins, A. Yu, L. Zhang and J. Zhang, *Energy Environ. Sci.*, 2011, **4**, 3167.

3. E. Negro and V. D. Noto, *J. Power Sources*, 2008, **178**, 634.
4. D.-W. Wang and D. Su, *Energy Environ. Sci.*, 2014, **7**, 576.
5. J. W. D. Ng, M. Tang and T. F. Jaramillo, *Energy Environ. Sci.*, 2014, **7**, 2017.
6. R. S. Figueiredo, R. Bertazzoli and C. A. Rodrigues, *Ind. Eng. Chem. Res.*, 2013, **52**, 5611.
7. H. T. Chung, J. H. Won and P. Zelenay, *Nat Commun*, 2013, **4**, 1922.
8. S. Siahrostami, A. Verdaguer-Casadevall, M. Karamad, D. Deiana, P. Malacrida, B. Wickman, M. Escudero-Escribano, E. A. Paoli, R. Frydendal, T. W. Hansen, I. Chorkendorff, I. E. L. Stephens and J. Rossmeisl, *Nat. Mater.*, 2013, **12**, 1137.
9. E. Brillas, I. Sires and M. A. Oturan, *Chem. Rev.*, 2009, **109**, 6570.
10. M. Nie, P.-K. Shen, M. Wu, Z.-D. Wei and H. Meng, *J. Power Source*, 2006, **162**, 173.
11. V. D. Noto, E. Negro, S. Polizzi, F. Agresti and G. A. Giffin, *ChemSusChem*, 2012, **5**, 2451.
12. A. Morozan, B. Jousselme and S. Palacin, *Energy Environ. Sci.*, 2011, **4**, 1238.
13. P. Chen, L.-K. Wang, G. Wang, M.-R. Gao, J. Ge, W.-J. Yuan, Y.-H. Shen, A.-J. Xie and S.-H. Yu, *Energy Environ. Sci.*, 2014, **7,** 4095.
14. W. He, C. Jiang, J. Wang and L. Lu, *Angew. Chem., Int. Ed.*, 2014, **53**, 9503.
15. P. Chen, T. Y. Xiao, Y. H. Qian, S. S. Li and S. H. Yu, *Adv. Mater.*, 2013, **25**, 3192.
16. H. A. Gasteiger and N. M. Markovic, *Science*, 2009, **324**, 48.
17. Y. Zheng, Y. Jiao, M. Jaroniec, Y. Jin and S. Z. Qiao, *Small*, 2012, **8**, 3550.
18. L. Feng, Y. Yan, Y. Chen and L. Wang, *Energy Environ. Sci.*, 2011, **4**, 1892.
19. K. Gong, F. Du, Z. Xia, M. Durstock and L. Dai, *Science*, 2009, **323**, 760.
20. L. Qu, Y. Liu, J.-B. Baek and L. Dai, *ACS nano*, 2010, **4**, 1321.
21. R. Bashyam and P. Zelenay, *Nature*, 2006, **443**, 63.
22. M. Lefevre, E. Proietti, F. Jaouen and J. P. Dodelet, *Science*, 2009, **324**, 71.
23. G. Wu, K. L. More, C. M. Johnston and P. Zelenay, *Science*, 2011, **332**, 443.
24. P. Chen, T.-Y. Xiao, Y.-H. Qian, S.-S. Li and S.-H. Yu, *Adv. Mater.*, 2013, **25**, 3192.
25. Q. Li, B. W. Noffke, Y. Wang, B. Menezes, D. G. Peters, K. Raghavachari and L.-s. Li, *J. Am. Chem. Soc.*, 2014, **136**, 3358.
26. M. S. A. Rahaman, A. F. Ismail and A. Mustafa, *Polym. Degrad. Stab.*, 2007, **92**, 1421.
27. B. Huskinson, M. P. Marshak, C. Suh, S. Er, M. R. Gerhardt, C. J. Galvin, X. D. Chen, A. Aspuru-Guzik, R. G. Gordon and M. J. Aziz, *Nature*, 2014, **505**, 195.
28. M. Shinohara, E. Araki, M. Mochizuki, T. Kanazawa and K. Suyehiro, *J. Power Sources*, 2009, **187**, 253.
29. Ø. Hasvold, T. Lian, E. Haakaas, N. Størkersen, O. Perelman and S. Cordier, *J. Power Sources*, 2004, **136**, 232.
30. X. Z. Fan, Y. H. Lu, H. B. Xu, X. F. Kong and J. Wang, *J. Mater. Chem.*, 2011, **21**, 18753.
31. H. B. Xu, X. Z. Fan, Y. H. Lu, L. A. Zhong, X. F. Kong and J. Wang, *Carbon*, 2010, **48**, 3300.
32. S. Pylypenko, A. Queen, T. S. Olson, A. Dameron, K. O'Neill, K. C. Neyerlin, B. Pivovar, H. N. Dinh, D. S. Ginley, T. Gennett and R. O'Hayre, *J. Phys. Chem. C*, 2011, **115**, 13667.
33. J. R. Pels, F. Kapteijn, J. A. Moulijn, Q. Zhu and K. M. Thomas, *Carbon*, 1995, **33**, 1641.

34. L. Laffont, M. Monthioux, V. Serin, R. B. Mathur, C. Guimon and M. F. Guimon, *Carbon*, 2004, **42**, 2485.

35. W. Shen, *Recent Patents on Chemical Engineering*, 2008, **1**, 27.

36. A. Achour, S. Vizireanu, G. Dinescu, L. Le Brizoual, M. A. Djouadi and M. Boujtita, *Appl. Surf. Sci.*, 2013, **273**, 49.

37. R. Silva, D. Voiry, M. Chhowalla and T. Asefa, *J. Am. Chem. Soc.*, 2013, **135**, 7823.

38. B. Cao, G. M. Veith, R. E. Diaz, J. Liu, E. A. Stach, R. R. Adzic and P. G. Khalifah, *Angew. Chem. Int. Ed.*, 2013, **52**, 10753.

39. R. M. Sellers, *The Analyst*, 1980, **105**, 950.

40. P. H. Matter, L. Zhang and U. S. Ozkan, *J. Catal.*, 2006, **239**, 83-96.

41. C. H. Choi, H.-K. Lim, M. W. Chung, J. C. Park, H. Shin, H. Kim and S. I. Woo, *J. Am. Chem. Soc.*, 2014, **136**, 9070.

42. Y. Lu, H. Xu, J. Wang and X. Kong, *Electrochimica Acta*, 2009, **54**, 3972.